IEEE Access
Multidisciplinary | Rapid Review | Open Access Journal

Received June 16, 2021, accepted July 9, 2021, date of publication July 20, 2021, date of current version August 5, 2021.

Digital Object Identifier 10.1109/ACCESS.2021.3098758

The Effect of Interfacial Zone Due to Nanoparticle–Surfactant Interaction on Dielectric Properties of Vegetable Oil Based Nanofluids

RIZWAN A. FARADE[1,2], NOOR IZZRI ABDUL WAHAB[1], (Senior Member, IEEE), DIAA-ELDIN A. MANSOUR[3], (Senior Member, IEEE), NORHAFIZ B. AZIS[1], (Senior Member, IEEE), JASRONITA BT. JASNI[1], (Senior Member, IEEE), VEERAPANDIYAN VEERASAMY[1], (Graduate Student Member, IEEE), ARANGARAJAN VINAYAGAM[4], (Member, IEEE), BANDANAWAZ M. KOTIYAL[2], AND T. M. YUNUS KHAN[5]

[1]Department of Electrical and Electronics Engineering, Faculty of Engineering, University Putra Malaysia, Serdang 43400, Malaysia
[2]Department of Electrical Engineering, School of Engineering and Technology, Anjuman-I-Islam's Kalsekar Technical Campus, Mumbai 410206, India
[3]Department of Electrical Power and Machines Engineering, Faculty of Engineering, Tanta University, Tanta 31511, Egypt
[4]Department of Electrical and Electronics Engineering, New Horizon College of Engineering, Bengaluru 560103, India
[5]Department of Mechanical Engineering, College of Engineering, King Khalid University, Abha 61421, Saudi Arabia

Corresponding authors: Rizwan A. Farade (rizwan.projects@gmail.com) and Noor Izzri Abdul Wahab (izzri@upm.edu.my)

The authors extend their appreciation to the Deanship of Scientific Research at King Khalid University for funding this work through Grant Number R.G.P. 1/251/42 and University Putra Malaysia under the under Grant GPB 9630000.

ABSTRACT Nanoparticles are generally anti-lipophilic and have a tendency to aggregate when they are embedded in nanofluids. Thus, surfactants have a major role in achieving long term dispersion stability of nanofluids through surface modification of nanoparticles. However, the surfactant changes the structure of the interfacial zone around nanoparticles and can have a crucial impact on the dielectric properties of dielectric nanofluids. Accordingly, this paper aims to clarify the role of interfacial zone on dielectric properties of vegetable oil based Al_2O_3 nanofluids including relative permittivity, dissipation factor, and AC breakdown voltage. Moreover, a polarization model of nanofluids was proposed to calculate their relative permittivity considering surfactant effect. Different filler levels ranging from 0.01 wt% to 0.05 wt% were used and various temperature ranges were considered to validate the proposed model. Relative permittivity calculated from the proposed model was almost in line with experimental results. Proposed model depicted that surfactant contributes for orientational polarization of nanoparticles in the relative permittivity calculation. So, improvement in the relative permittivity of dielectric nanofluids has been attained from 0.01 wt% to 0.05 wt% of Al_2O_3 nanoparticles due to both internal and orientational polarization of nanoparticles. Regarding dissipation factor of prepared nanofluids, it decreased against the weight percentage of nanoparticles, while the mean AC breakdown voltage increased against the weight percentage. All these effects were discussed considering the structure of interfacial zone and its impact on the alignment of oil chains and the energy loss of electrons.

INDEX TERMS Al_2O_3 nanoparticles, surfactant, relative permittivity model, nanofluids, dielectric properties.

NOMENCLATURE

2a	Diameter of spherical nanoparticle
CSO	Cottonseed oil
d	Surfactant thickness
DBF	Dielectric base fluid
DNF	Dielectric nanofluid
dQ	Charge on nanoparticle's small volume
E_0	External electric field applied in the direction of x-axis

The associate editor coordinating the review of this manuscript and approving it for publication was Abhishek K. Jha.

k	Boltzmann constant
N_1	Number of base oil molecules/unit volume
N_2	Number of nanoparticle molecules/unit volume
NP	Nanoparticle
p	Electric dipole moment of nanoparticles
SDBS	Sodium Dodecylbenzene Sulfonate
T	Temperature
TBHQ	Tertiary Butylhydroquinone
V	Volume of each nanoparticle
α_1	Polarizability of base oil molecules
α_2	Inner polarizability of NPs
α_3	Orientational polarizability of charged NPs
ε_0	Permittivity of vacuum
ε_{NF}	Relative permittivity of DNF
ε_1	Relative permittivity of base fluid
ε_2	Relative permittivity of NPs
φ_{NP}	Volume fraction of NPs in DNF
σ_1	Charge density of NPs without surfactant polarization
σ_2	Charge density of NPs with surfactant polarization

I. INTRODUCTION

Power transformers can be classified as small, medium and large power transformers based on their ratings. Power transformers are generally liquid cooled and use billions of litres of transformer oil. Distribution transformer units are more numerous and therefore consume more transformer oil than other power transformers. The demand for transformer oil is increasing every day. The increase in energy consumption is a key factor in the increasing demand for transformer oil. Mineral oils are the conventional transformer oil those are currently used in the majority of transformer applications. Environmental concerns and the non-renewable nature of mineral oils shifted paradigm to vegetable oil dielectrics [1], [2].

With the advancement in nanotechnology, the concept of nanofluids has been widely developed to improve various properties of the base fluids. For dielectric fluids, the constituted nanofluids can be denoted as DNFs. Recent studies showed that stably dispersed nanoparticles into DBFs improves dielectric properties of DNFs to a considerable extent [3]–[9]. These improvements are attributed to repeated trapping and de-trapping of charge carriers into the fluid causing a limit in the transportation of these charge carriers under the influence of electric field. In the continuous media these traps are generally made by chemical defects [10], in case of natural esters these traps are due to carbonyl groups. In DNFs, additional trapping sites are formed by NPs due to the difference in the relative permittivity of NPs and that of base oil [11].

Several models have been proposed to calculate the relative permittivity of these composite fluids. In this regard, the Maxwell-Garnett model was widely used in the description and measurement of the relative permittivity of DNFs [12], but this model is not considered being sufficient since it is just a function of the concentration and relative permittivities of the constituents. As a result, a model was constructed in [13] based on S-parameter retrieval and considering the scattering of nanoparticles. The S-parameter retrieval model could estimate more accurate relative permittivity than that obtained from the Maxwell-Garnett model. Moreover, a proposed model based on NP polarization was proposed to investigate the relative permittivity of composite fluids [14], and could exhibit more closer results to the experimental ones. However, all these models [12]–[14] did not consider the surfactant polarization.

NPs are generally anti-lipophilic and have a tendency to aggregate when they are embedded in nanofluids. Thus, using of surfactants became a major process in achieving long term dispersion stability of nanofluids through surface modification of nanoparticles [15], [16]. In [17], the effect of surfactant amount on stabilization of nanoparticles were clarified and it was concluded that excess amount of surfactant can hinder stability due to the formation of double surfactant chains around the surface of nanoparticles. This concept was effectively utilized in [18], where the usage of suitable surfactant amount could enhance the dispersion behavior of TiO_2 nanoparticles into transformer oil with a positive impact on the breakdown strength. The usage of surfactant with various ultrasonication periods were investigated in [19] and it was found that the longer the ultrasonication period up to optimized period, the higher the UV-Vis absorbance and the more homogenous the dispersion of nanoparticles.

Regarding the effect of surfactant on long term stability, it was discussed in [20] and [21]. In [20], aluminium nitride nanoparticles were modified with two layers of surfactants before dispersion into the transformer oil. This modification enabled to keep the stability of the prepared nanofluids more than 6 months with an enhancement up to 7% in thermal conductivity and up to 50% in positive lightning impulse breakdown. In [21], the oleic acid was used as a surfactant with iron oxide nanoparticles to fill the transformer oil and prepare what is called magnetic nanofluids. The stability of these magnetic nanofluids was measured over 7 years.

In addition to the role of surfactant in keeping long term stability, it was found that it plays an important role in strengthening the interfacial zone around nanoparticles. This interfacial zone is considered to have a major impact on the dielectric properties of nanofluids [22], like its significance in solid nanodielectrics as reported by many researchers [23]–[25]. Since surfactants are frequently used to keep long term stability and to strengthen the interfacial zone, it is crucial to consider the surfactant polarization in the relative permittivity calculation of nanofluids.

This research focuses on to clarifying the role of interfacial zone on dielectric properties of CSO based Al_2O_3 nanofluids. The effect of surfactant polarization on relative permittivity of CSO based Al_2O_3 nanofluids is also clarified. Cottonseed oil is a non-edible vegetable oil that represents a promising candidate to replace conventional mineral oil. Detailed characterization of Al_2O_3 nanoparticles and methodology

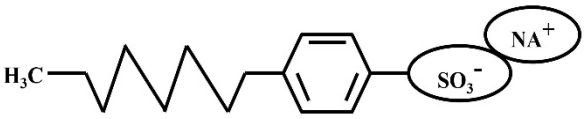

FIGURE 1. Chemical structure of SDBS.

adopted for the preparation of nanofluids were presented. Experimental relative permittivity results of DNFs at different concentrations (Viz., 0.01 wt%, 0.02 wt%, 0.03 wt%, and 0.05 wt%) and varying temperature (Viz., 45 °C, 60 °C, 75 °C and 90 °C) were investigated and compared. A relative permittivity model of composite fluids considering surfactant polarization was proposed. Relative permittivity model results were compared with experimental relative permittivity results. Effect of interfacial zone on improved relative permittivity, AC breakdown voltage and dissipation factor were discussed with the help of experimental results.

II. MATERIALS AND METHODOLOGY

A. MATERIALS

Al_2O_3 NPs were procured from Nanopar Tech, Chandigarh, India. The bulk density of the Al_2O_3 NPs was 0.18 g/mL, with a large surface area, morphology of nearly spherical, and a purity of 99.99%. SDBS was used as a surfactant, since it proved an enhanced stability when being used with Al_2O_3-water nanofluids [26]. It was purchased from Sigma-Aldrich, India, and has the formula of $CH_3(CH_2)_{11}C_6H_4SO_3^-NA^+$ with the structure shown in Fig. 1. Pure, natural and cold pressed cottonseed oil was extracted from cottonseeds purchased from the local Indian market. TBHQ was used as a synthetic antioxidant and it was purchased from Sigma-Aldrich, India. The typical values for physical and chemical properties of cottonseed oil can be found in [27]. Cold pressed cottonseed oil was selected in the current implementation for two reasons. First, cold pressing can retain higher levels of natural antioxidants that may be lost during the refining steps of a commercially available cottonseed oil. Second, cold pressing uses no organic solvent, resulting in chemically contaminant-free oil [28].

B. PREPARATION OF Al_2O_3 NANOFLUIDS

In the current investigation, the cold pressed CSO was used. Preparation of CSO as DBF was already presented in our prior studies [29], [30]. Same procedure was adopted in the current implementation. The cold pressed CSO was introduced with TBHQ (0.02%) and then the solution was heated at 80°C for 90 minutes by magnetic stirrer, thereby removing water and gas contaminants from the oil. Thus, the CSO as DBF became ready for the current implementation. Measured quantities of Al_2O_3 NPs and SDBS surfactant were introduced into CSO DBF and stirred for 20 minutes at room temperature to form DNFs. Al_2O_3 NPs were introduced at 0.01 wt%, 0.02 wt%, 0.03 wt%, and 0.05 wt%, with a 1:1 ratio of SDBS surfactant to Al_2O_3 NPs. The maximum weight fraction of Al_2O_3 NPs was 0.05 wt%, since it has proved stable suspension in natural ester oil [31].

Stable dispersion of DNF samples were attained by Probe Sonicator (Model: PKS-250FM, Anamatrix Instrument Technologies Private Limited, Bangalore, India), with sonication time of 30 minutes at power setting of 50% and pulse setting of 40%. Stability analysis of prepared nanofluids was carried out by visual inspection over a period of four weeks. Nanofluids showed stable dispersion without any aggregates. Fig. 2a includes visual image of Al_2O_3 powder sample and Fig. 2b includes visual images of prepared DNFs (Viz., 0.01 wt%, 0.02 wt%, 0.03 wt%, and 0.05 wt%). Furthermore, to assure the reliability of the obtained results, the dielectric properties were measured shortly after preparation.

III. CHARACTERIZATION OF Al_2O_3 NPs

Fig. 3a and b show transmission electron microscope (TEM, Model: JEM 2100 PLUS, JEOL Ltd., Tokyo, Japan) images of aluminium oxide nanoparticles at different magnification levels. These figures illustrate an aggregate phenomenon of the nanoparticles with a primary particle size of 15-25 nm (±0.5 nm). Selective Area Electron Diffraction (SAED) pattern is shown in Fig. 3c, in which numerous discrete spots line-up and form rings indicating polycrystalline structure. High-resolution TEM image in Fig. 3d indicates multiple planes of different crystals oriented in different directions.

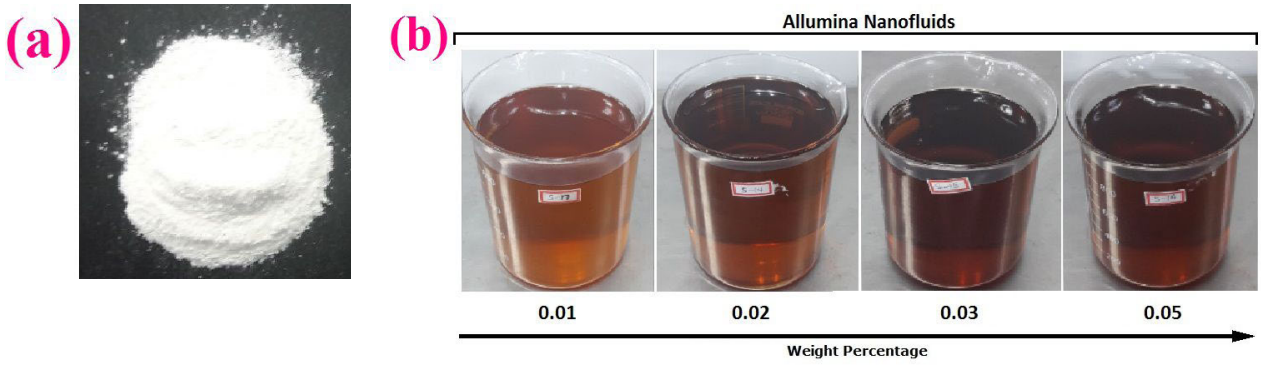

FIGURE 2. Visual images of: (a) Al_2O_3 powder, and (b) Prepared Al_2O_3 nanofluids.

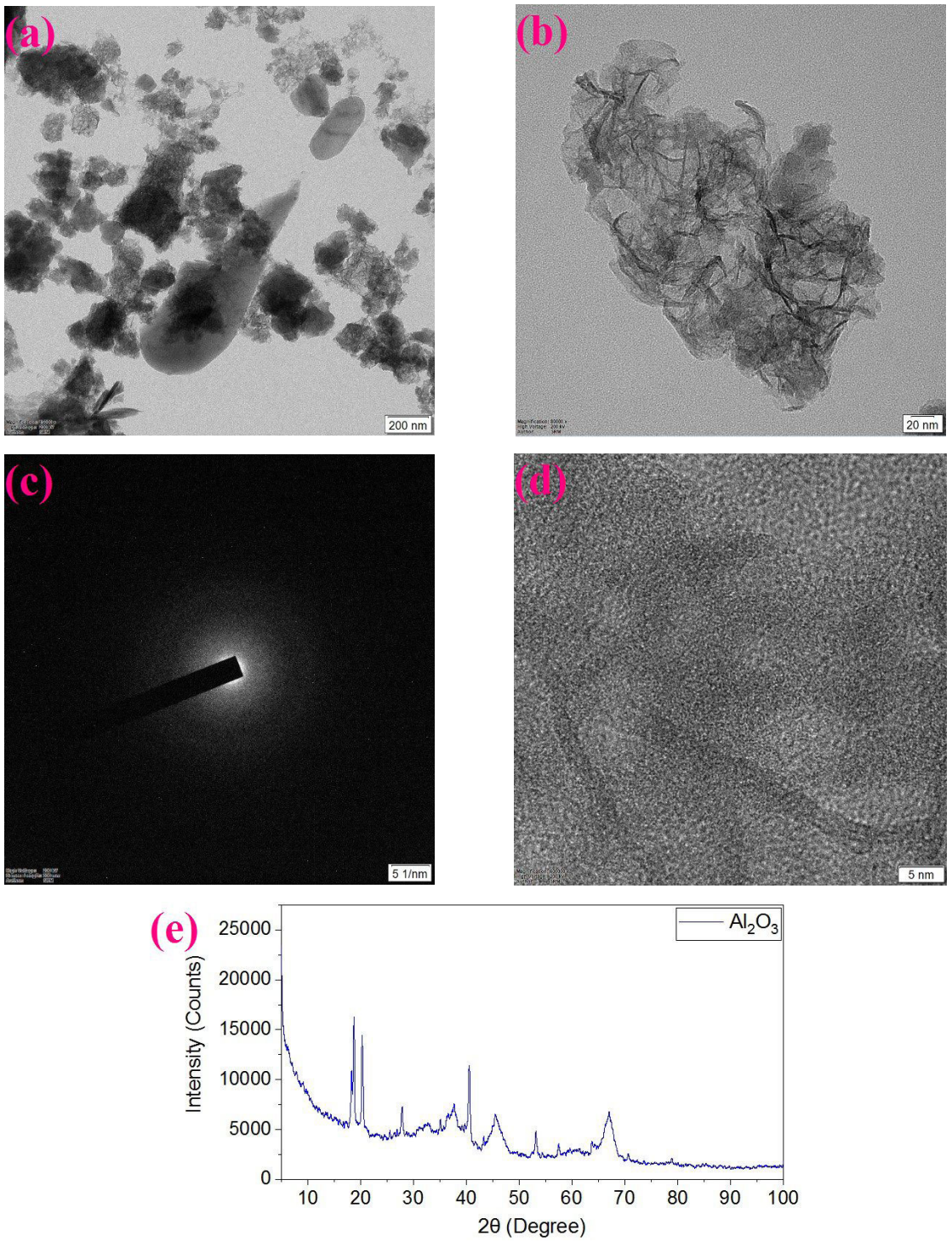

FIGURE 3. Al_2O_3 nanoparticles: (a) TEM image at magnification level 15000 x; (b) TEM image at magnification level 80000 x; (c) SAED pattern; (d) High-resolution TEM image; and (e) XRD pattern.

The X-ray diffraction (XRD, Model: SmartLab SE, Rigaku Corporation, Tokyo, Japan) was obtained for the powder in the 2θ range (0° - 100°) and its pattern is displayed in Fig. 3e. The sharp peaks in XRD pattern ensure Al_2O_3 with crystalline structure. From XRD data, the area of crystalline peaks was calculated as 145082 square units and the total area of all peaks was calculated as 238152 square units, thus the degree of crystallinity was found to be 60.92% referring to the following equation:

$$\text{Crystallinity} = \frac{\text{Area of crystalline peaks}}{\text{Total area}} \times 100 \qquad (1)$$

IV. RELATIVE PERMITTIVITY EXPERIMENTAL RESULTS

The relative permittivity or dielectric constant of a dielectric is an AC characteristic and is defined as the increase in capacitance/stored charge, by means of a dielectric medium. The increase in the capacitance/stored charge is attributable to the polarization of the dielectric by the applied electric field [32], as explained in the subsequent section. The relative permittivity of insulating oil in contact with cellulose insulation can affect the local voltage stress distribution. The higher the relative permittivity of oil, the closer its value to that of cellulose insulation and the higher the improvement in electrical stress distribution. Relative permittivity of prepared Al_2O_3 DNFs was measured at various temperatures with ADTR 2K Plus (ELTEL Industries, Bangaluru, India) automatic test set in accordance with the IEC 60247 standard. Relative permittivity was measured at 500 V and 50 Hz AC. Fig. 4 shows the relative permittivity of Al_2O_3 DNFs at different filler levels (Viz., 0.01 wt%, 0.02 wt%, 0.03 wt%, and 0.05 wt%) at four temperature ranges (Viz., 45 °C, 60 °C, 75 °C and 90 °C).

As observed from Fig. 4 the relative permittivity of Al_2O_3 DNFs at a given temperature increases with the increase in the weight percentage from 0.01 wt% to 0.05 wt%. At 45 °C, the relative permittivity increases from 2.98 to 3.87 with the increase in weight percentage from 0.01 wt% to 0.05 wt%. The relative permittivity of Al_2O_3 DNFs at a given weight percentage is also a function of the temperature, where it decreases with the increase in temperature. The temperature dependency of relative permittivity has similar trend to that obtained in literature [29], [33], [34]. The relative permittivity at 45 °C was measured as 2.98, 3.21, 3.44, and 3.87 for 0.01 wt%, 0.02 wt%, 0.03 wt%, and 0.05 wt% DNFs, respectively. Whereas, at 90 °C for the same DNFs, it was measured as 2.83, 2.99, 3.21, and 3.67, respectively.

The increase in the relative permittivity of DNFs with the increase in weight percentage of Al_2O_3 NPs can be attributed to internal polarization of NPs and orientational polarization of charged NPs referring to the Clausius-Mossotti equation as follows:

$$\frac{\varepsilon_{NF}-1}{\varepsilon_{NF}+2}=\frac{1}{3\varepsilon_0}[N_1\alpha_1+N_2\alpha_2+N_2\alpha_3] \tag{2}$$

As both internal polarization of NPs and orientational polarization of charged NPs increase with the increase in the number of nanoparticles, so the relative permittivity increases against the weight percentage of NPs. The decreasing trend in relative permittivity with the increase in temperature at each weight percentage of Al_2O_3 NPs was observed and was justified with the proposed model in the next section.

V. RELATIVE PERMITTIVITY MODEL WITH SURFACTANT CONSIDERATION

DNFs under the influence of an external electrical field, both base oil molecules and NPs will get polarized. Surface polarization charges (positive and negative) are accumulated

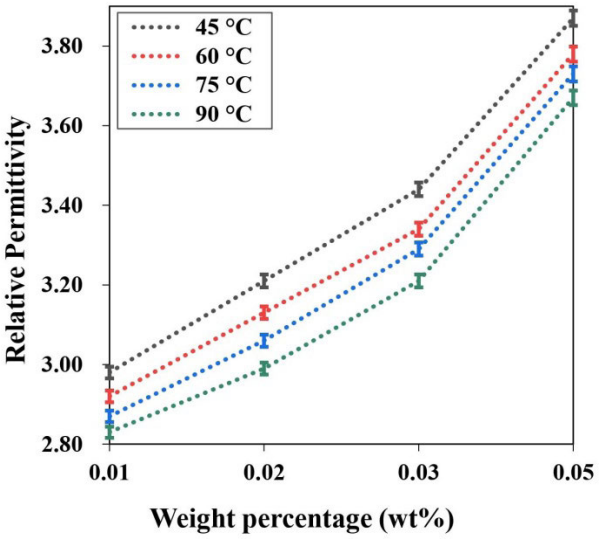

FIGURE 4. Experimental relative permittivity results of Al_2O_3 nanofluids at varying temperatures and weight percentages.

on either sides of the nanoparticle, resulting in the particle being charged. There are three types of polarization in DNFs that determine the relative permittivity of DNF, as well as the local voltage stress distribution under external electrical field. Namely, polarization of base fluid molecules, internal polarization of NPs, and orientational polarization of charged NPs. Clausius-Mossotti equation expresses the relative permittivity of DNFs in terms of polarization as depicted above in equation (2).

Equation (2) can be expressed as follows:

$$\frac{\varepsilon_{\mathrm{NF}}-1}{\varepsilon_{\mathrm{NF}}+2}=\frac{\mathrm{N}_1\alpha_1}{3\varepsilon_0}+\frac{\mathrm{N}_2\alpha_2}{3\varepsilon_0}+\frac{\mathrm{N}_2\alpha_3}{3\varepsilon_0} \tag{3}$$

For the pure dielectric fluid (without nanoparticle), equation (3) is simplified as follows:

$$\frac{\varepsilon_1-1}{\varepsilon_1+2}=\frac{\mathrm{N}_1\alpha_1}{3\varepsilon_0} \tag{4}$$

By definition, polarizability of NPs can be expressed as follows [32]:

$$\alpha_2=\varepsilon_0\left(\varepsilon_2-1\right)\mathrm{V} \tag{5}$$

Assume nanoparticles are spherical, the number of nanoparticles per unit volume can be calculated as follows:

$$N_2=\frac{\varphi_{NP}}{V}=\frac{\varphi_{NP}}{\frac{4}{3}\Pi a^3}=\frac{3\varphi_{NP}}{4\Pi a^3} \tag{6}$$

From equations (5) and (6), the following equation can be obtained:

$$\frac{N_2\alpha_2}{\varepsilon_0}=\varphi_{NP}\left(\varepsilon_2-1\right) \tag{7}$$

The charge density of NPs surface polarization excluding surfactant polarization can be expressed as follows [14]:

$$\sigma_1=\varepsilon_0E_0\left(\frac{\varepsilon_2-\varepsilon_1}{\varepsilon_2+2\varepsilon_1}\right)\sin\theta\cos\varphi \tag{8}$$

To consider surfactant polarization under an external electric field, the polarization model in Fig. 5 is proposed. The polarization charges, including positive and negative charges, are accumulated on both sides of the spherical NP and opposite to the external electrical field as shown in Fig. 5a. As a result, surfactant encapsulates NP with opposite polarization charges on the inner side to neutralize net charges of NP. While on the outer side, same amount of opposite charges gets distributed. Fig. 5b shows the same polarization NP model with illustrating all dimensions of NP and surfactant as well as the magnitude of polarization charges.

Considering surfactant polarization, surface charge density on NP can be expressed as follows [16]:

$$\sigma_2 = \varepsilon_0 E_0 \left[\left(\frac{\varepsilon_2 - \varepsilon_1}{2\varepsilon_1 + \varepsilon_2}\right) - \left(\frac{ad + d^2}{a}\right)\left(\frac{\varepsilon_2 - \varepsilon_1}{2\varepsilon_1 + \varepsilon_2}\right)\right] \times \sin\theta \cos\varphi \quad (9)$$

Referring to Fig. 6 and considering surfactant polarization, the total positive charge (Q_+) on NPs can be calculated as follows:

$$dQ = \sigma_2 a\, d\theta\, a\, \sin\,\theta\, d\varphi \quad (10)$$

$$Q_+ = 4.\int_0^{\Pi/2}\int_0^{\Pi/2} \sigma_2 a^2 \sin\,\theta\, d\theta\, d\varphi \quad (11)$$

$$Q_+ = \Pi a^2 \varepsilon_0 E_0 \left[\left(\frac{\varepsilon_2 - \varepsilon_1}{2\varepsilon_1 + \varepsilon_2}\right) - \left(\frac{ad + d^2}{a}\right)\left(\frac{\varepsilon_2 - \varepsilon_1}{2\varepsilon_1 + \varepsilon_2}\right)\right] \quad (12)$$

According to the dielectric concept of polar molecules, the electric dipole moment of NPs molecules can be expressed as follows:

$$\mathrm{p} = 2\mathrm{a}\, Q_+ \quad (13)$$

Dipolar orientational polarizability α_3 per molecule can be defined as follows:

$$\alpha_3 = \frac{p^2}{3kT} = \frac{4a^2 Q_+^2}{3kT} \quad (14)$$

Substituting the value of Q_+ in equation (14), the following equation can be obtained:

$$\alpha_3 = \frac{4a^6}{3kT}\Pi^2 \varepsilon_0^2 E_0^2 \times \left[\left(\frac{\varepsilon_2 - \varepsilon_1}{2\varepsilon_1 + \varepsilon_2}\right) - \left(\frac{ad + d^2}{a}\right)\left(\frac{\varepsilon_2 - \varepsilon_1}{2\varepsilon_1 + \varepsilon_2}\right)\right]^2 \quad (15)$$

Thus, substituting fourth term of equation (6) and (15), the third term in equation (2) can be expressed as follows:

$$\frac{N_2\alpha_3}{\varepsilon_0} = \frac{1}{kT}\Pi\varepsilon_0 a^3 \varphi_{NP} E_0^2 \times \left[\left(\frac{\varepsilon_2 - \varepsilon_1}{2\varepsilon_1 + \varepsilon_2}\right) - \left(\frac{ad + d^2}{a}\right)\left(\frac{\varepsilon_2 - \varepsilon_1}{2\varepsilon_1 + \varepsilon_2}\right)\right]^2 \quad (16)$$

Substituting for equations (4), (7), and (16) into equation (2), the polarization model of DNF considering surfactant polarization can be obtained as follows:

$$\frac{\varepsilon_{NF} - 1}{\varepsilon_{NF} + 2} = \frac{\varepsilon_1 - 1}{\varepsilon_1 + 2} + \frac{\varphi_{NP}(\varepsilon_2 - 1)}{3} + \frac{1}{3kT}\Pi\varepsilon_0 a^3 \varphi_{NP} E_0^2 \times \left[\left(\frac{\varepsilon_2 - \varepsilon_1}{2\varepsilon_1 + \varepsilon_2}\right) - \left(\frac{ad + d^2}{a}\right)\left(\frac{\varepsilon_2 - \varepsilon_1}{2\varepsilon_1 + \varepsilon_2}\right)\right]^2 \quad (17)$$

TABLE 1. Parameters considered in calculating the relative permittivity of nanofluids according to the proposed model.

No.	Parameter	Value
1	2a	20 nm
2	D	1.5 nm
3	ε_1	2.941 at 45 °C, 2.879 at 60 °C, 2.84 at 75 °C and 2.799 at 90 °C
4	ε_2	7.8
5	ε_0	$8.854187817 \times 10^{-12}$ F.m^{-1}
6	φ_{NP}	0.01 wt%, 0.02 wt%, 0.03 wt%, and 0.05 wt%
7	k	1.380649×10^{-23} J·K^{-1}
8	T	318.15 K, 333.15 K, 348.15 K, and 363.15 K.

VI. COMPARISON OF THE PROPOSED MODEL WITH EXPERIMENTAL RELATIVE PERMITTIVITY RESULTS

In this section, the proposed model in the previous section is compared to the experimental results. As indicated from TEM images in Section III, primary particle size of Al_2O_3 was in the range from 15 to 25 nm. To calculate relative permittivity of DNFs according to the proposed model, the average diameter of NPs is considered 20 nm, the thickness of surfactant is considered 1.5 nm [16], and the external electric field applied is 500 V. Other parameters are depicted in Table 1.

Comparison between results of the proposed model and experimental results at 45 °C, 60 °C, 75 °C, and 90 °C are depicted in Fig. 7. The values of relative permittivity calculated are in good agreement with that obtained experimentally. At a given temperature and weight percentage, there is a slight difference between the results obtained from the model and the experimental results. The percentage difference between the experimental results and the model results are depicted in Table 2, lowest difference is 3.48% and highest difference is 6.16%. Accordingly, the developed model will enable to accurately calculate the gross relative permittivity of nanofluids before actual development.

VII. EXPERIMENTAL RESULTS OF TAN δ

The relative magnitude of dielectric loss with respect to dielectric constant is defined as tan δ. It is also called the loss factor (or loss tangent). The tan δ of prepared Al_2O_3 DNFs was measured at various temperatures with ADTR 2K Plus (ELTEL Industries, Bangaluru, India) automatic test set in accordance with the IEC 60247 standard. Tan δ is an AC characteristic and was measured at 500 V and 50 Hz AC. Fig. 8 shows the tan δ of Al_2O_3 DNFs at different filler

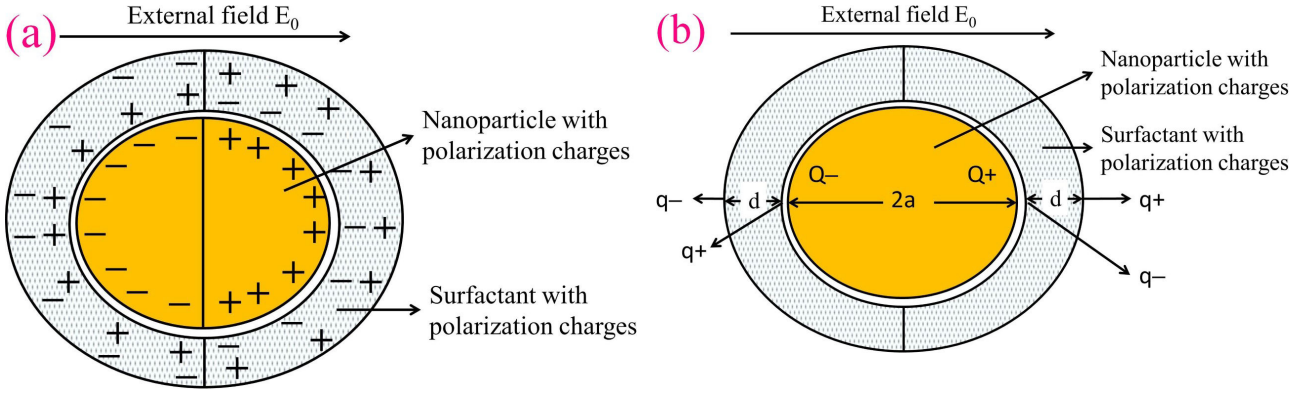

FIGURE 5. Polarization model of nanoparticle post electrical field application on nanofluid (a) Polarization charges; and (b) Dimensions and charge magnitude of nanoparticle and surfactant.

TABLE 2. Experimental and model result percentage difference.

Temperature → wt% ↓	45 °C	60 °C	75 °C	90 °C
0.01	4.87 %	4.99 %	5.36 %	5.28 %
0.02	3.88 %	4.39 %	5.29 %	6.16 %
0.03	3.48 %	4.36 %	4.45 %	5.44 %
0.05	5.03 %	5.33 %	5.17 %	5.22 %

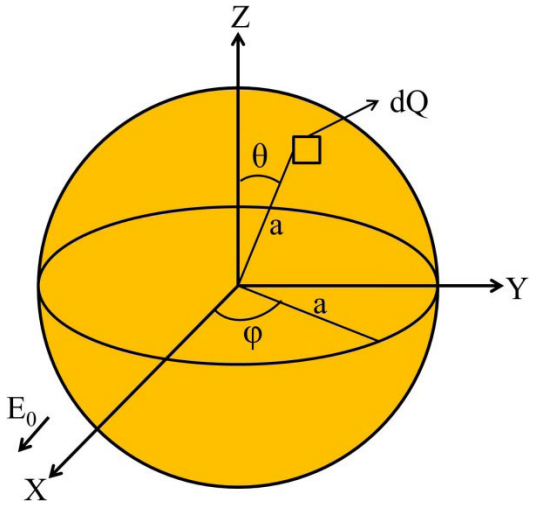

FIGURE 6. Surface polarization charges on nanoparticle post electrical field application on nanofluid.

levels (Viz., 0.01 wt%, 0.02 wt%, 0.03 wt%, and 0.05 wt%) and at four temperature ranges (Viz., 45 °C, 60 °C, 75 °C and 90 °C).

As observed from Fig. 8, the tan δ of Al_2O_3 DNFs at a given temperature decreases with the increase in the weight percentage from 0.01 wt% to 0.05 wt%. At 45 °C, tan δ decreases from 0.043 to 0.016 with the increase in weight percentage from 0.01 wt% to 0.05 wt%. The tan δ of Al_2O_3 DNFs is also a function of temperature at a given weight percentage. In fact, tan δ increases with the increase in temperature which is in line with the literature [35]. At 0.01 wt%, the tan δ increases from 0.043 to 0.1656 with the increase in temperature from 45 °C to 90 °C, while at 0.05 wt%, the tan δ increases from 0.016 to 0.0716 with the same increase in temperature.

The decrease in tan δ of DNFs with the increase in weight percentage of Al_2O_3 NPs is attributed to the increase of dielectric constant and the decrease of dielectric loss in the denominator and numerator of tan δ, respectively. For dielectric constant, it increases with the increase in weight percentage due to the increase in number of Al_2O_3 NPs as discussed in the earlier section. On the other hand, the charge trapping provided by nanoparticles and their interfaces decreases the dielectric loss [29]. Thus, the total effect is the decrease of tan δ against the weight percentage. This decrease in tan δ against the weight percentage is more pronounced at 90 °C than that at 45 °C. This trend can be attributed to the effect of temperature on the number of charge carriers into the fluid and Brownian motion of nanoparticles. Increasing the temperature causes an increase in the number of charge carriers, thereby increasing the value of dielectric loss and tan δ. On the other hand, increasing the temperature causes a subsequent increase in Brownian motion of nanoparticles enabling to trap more charge carriers, thereby decreasing the value of dielectric loss and tan δ. With increasing the weight percentage of nanoparticles, the temperature effect on Brownian motion increases, while the temperature effect on the number of charge carriers remains constant, causing the decrease in tan δ against the weight percentage to be more pronounced at 90 °C.

VIII. AC BREAKDOWN VOLTAGE EXPERIMENTAL RESULTS

AC breakdown voltage measures the ability of transformer oil to withstand high voltages during real-time application. AC BDV of DNFs was measured as per IEC 60156, whose specifications include sphere to sphere electrode, 2.5 mm gap and 2 kV/s voltage ramp rate. The mean value of AC BDV for the DBF at room temperature and pressure was measured as 37.6 kV.

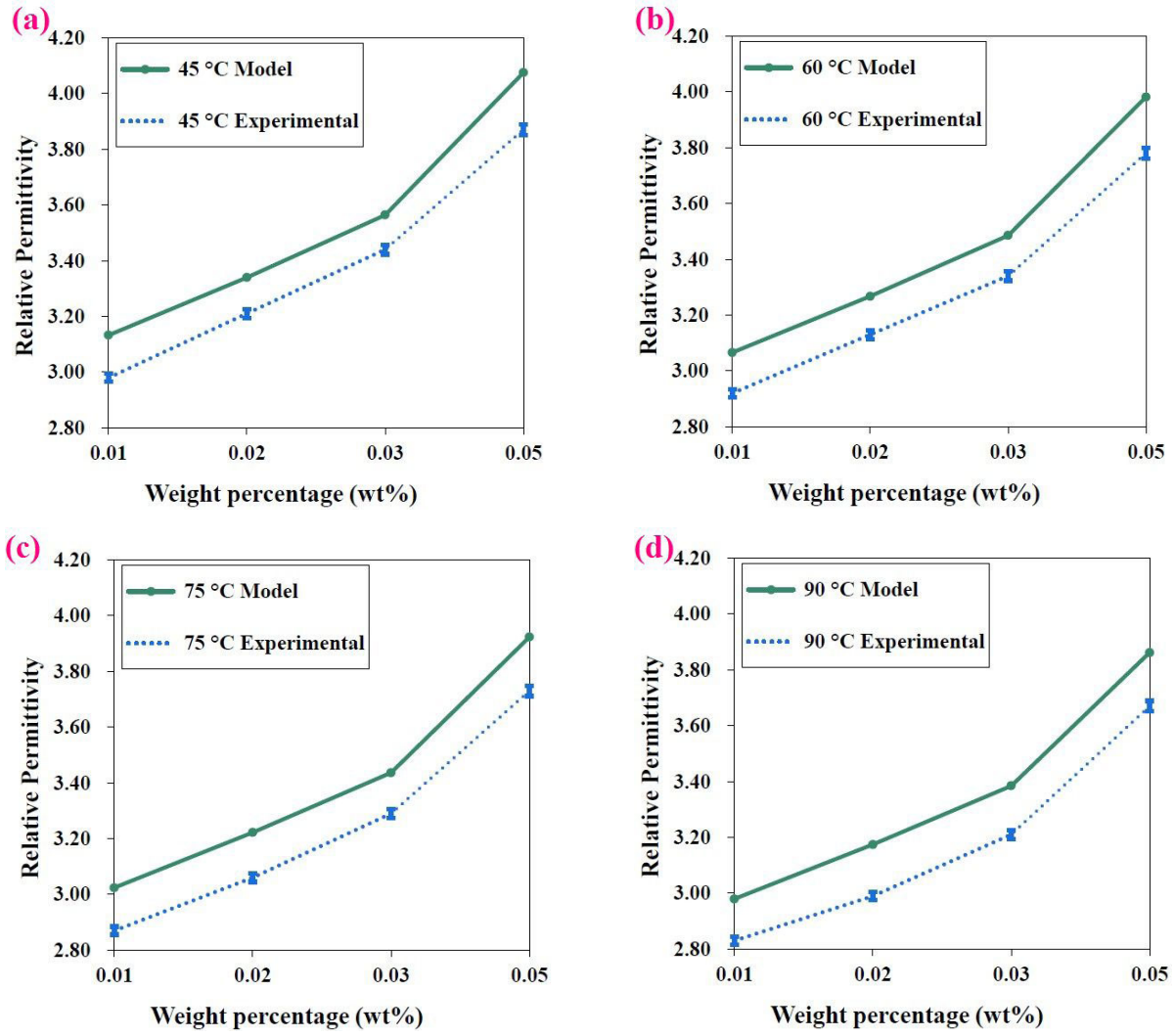

FIGURE 7. Relative permittivity of nanofluids according to the proposed model at various temperatures: (a) 45 °C, (b) 60 °C, (c) 75 °C and (d) 90 °C.

The mean AC BDV of Al_2O_3 DNFs is incremental with the weight percentage of Al_2O_3 NPs (Viz., 0.01 wt%, 0.02 wt%, 0.03 wt% and 0.05 wt%) as depicted in Fig. 9. This increment is attributed to the increase in trapping depth provided by the increase in weight percentage of Al_2O_3 NPs. Maximum AC BDV was measured at 0.05 wt% of Al_2O_3 DNF and it was measured as 46.2 kV corresponding to a percentage enhancement of about 23%. Mean, standard deviation (SD), and percentage enhancement in AC BDV of DNFs is listed in Table 3.

TABLE 3. AC BDV test results of Al_2O_3 DNFs.

Sample (wt %)	AC BDV		
	Mean (kV)	SD	Enh. (%)
0.01	41.8	2.15	11.17
0.02	43.3	1.91	15.15
0.03	44.8	2.71	19.14
0.05	46.2	2.85	22.87

IX. DISCUSSION

A. INTERFACIAL ZONE

It is known that Al_2O_3 nanoparticles absorbs H+ or OH- species by water absorbance from moisture existing in the oil. This depends upon acid-base equilibrium which is determined by the isoelectric point of nanoparticles and pH of base oil. The isoelectric point is a point at which nanoparticles carriers no net charges on their surface. Since pH value of cottonseed oil is around 7 [36] and the isoelectric point of Al_2O_3 is 9.4 [37], Al_2O_3 nanoparticles absorb H+ species on O atoms and get positive charges on their surface. Accordingly, the usage of an anionic surfactant like SDBS facilitates its adsorption on the surface of nanoparticles leaving behind

TABLE 4. Relative permittivity due to orientational polarization.

wt% ↓	45 °C ↓		60 °C ↓		75 °C ↓		90 °C ↓	
	Without	With	Without	With	Without	With	Without	With
0.01	6.65×10^{-13}	1.49×10^{-14}	6.64×10^{-13}	3.49×10^{-13}	6.52×10^{-13}	3.43×10^{-13}	6.44×10^{-13}	3.38×10^{-13}
0.02	1.33×10^{-12}	6.99×10^{-13}	3.32×10^{-12}	6.98×10^{-13}	1.30×10^{-12}	6.86×10^{-13}	1.29×10^{-12}	6.77×10^{-13}
0.03	2.00×10^{-12}	1.05×10^{-12}	1.99×10^{-12}	1.05×10^{-12}	1.96×10^{-12}	1.03×10^{-12}	1.93×10^{-12}	1.02×10^{-12}
0.05	3.33×10^{-12}	1.75×10^{-12}	3.32×10^{-13}	1.74×10^{-12}	3.26×10^{-12}	1.72×10^{-12}	3.22×10^{-12}	1.69×10^{-12}

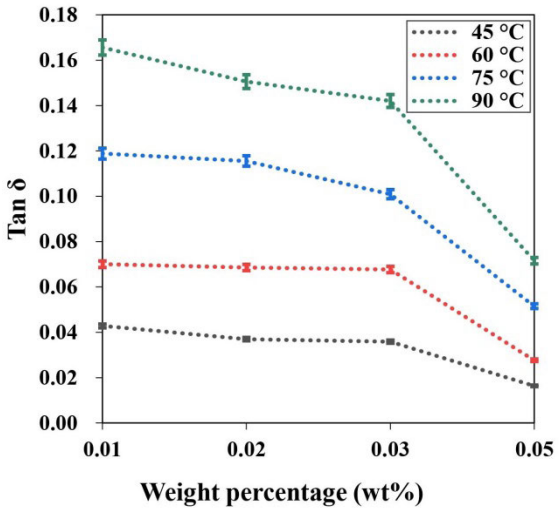

FIGURE 8. Tan δ of Al_2O_3 nanofluids at varying temperatures and weight percentages.

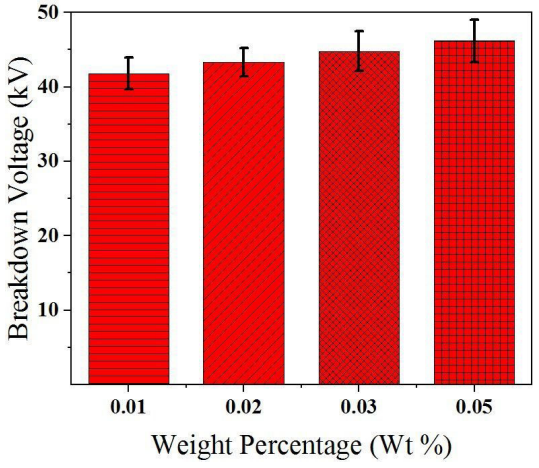

FIGURE 9. AC BDV test results of Al_2O_3 DNFs.

NaOH as shown in Fig. 10. This results in a sufficient repulsion force between nanoparticles and an enhancement in the dispersion of nanoparticles with positive impacts on thermal and dielectric properties.

B. IMPACT OF INTERFACIAL ZONE ON DIELECTRIC PROPERTIES

Since, surfactants' heads are adsorbed on the surface of nanoparticles and their tails are directed towards oil, surfactants' molecules become aligned in parallel to each other and perpendicular to the surface of nanoparticles. The intermolecular forces keep the molecules staying apart from each other. As a result, oil chains in this region are forced to be aligned between surfactants' molecules creating two different layers [38] as shown in Fig. 11. The first layer is the aligned layer where oil chains are arranged perpendicular to nanoparticle surface and parallel to surfactants' molecules. The second layer is the affected layer, which has less aligned oil chains but is affected by the first layer. In case of nanofluids without surfactant there will be only the affected layer due to confinement of oil chains in the vicinity of nanoparticles at the interfacial zone.

For nanofluids with SDBS surfactant, the obtained dielectric properties are referred to interfacial zone. As mentioned above the interfacial zone is composed of two different layers. The aligned layer has a rigid structure that is difficult to polarize. Due to this rigid structure, the total amount of polarization decreases resulting in a decrease of dielectric constant with the addition of surfactant. This rigid structure also makes it easy for electrons to lose their energy resulting in an increase in breakdown strength and a decrease in dielectric losses.

C. COMPARISON OF PROPOSED MODEL FOR SURFACTANT TREATED AND NON-TREATED NANOPARTICLES

Referring to proposed model, the first and second terms on the right hand side of equation (17) represent relative permittivity contribution by polarization of base oil molecules and inner polarization of nanoparticles, respectively, while the third term represents relative permittivity contribution by orientational polarization. Therefore, the first and second terms remain the same for nanoparticles either treated with surfactant or non-treated without surfactant. Whereas, the third term changes for nanoparticles treated with and without surfactant. Table 4 shows relative permittivity contribution due to orientational polarization with and without surfactant at different filler levels (Viz., 0.01 wt%, 0.02 wt%, 0.03 wt%, and 0.05 wt%) and at four temperature ranges (Viz., 45 °C, 60 °C, 75 °C and 90 °C). It is worthy mentioned that the relative permittivity contribution without surfactant calculated by the present proposed model matches well with the model proposed earlier in [14]. This validates the proposed model. However, the current research presents

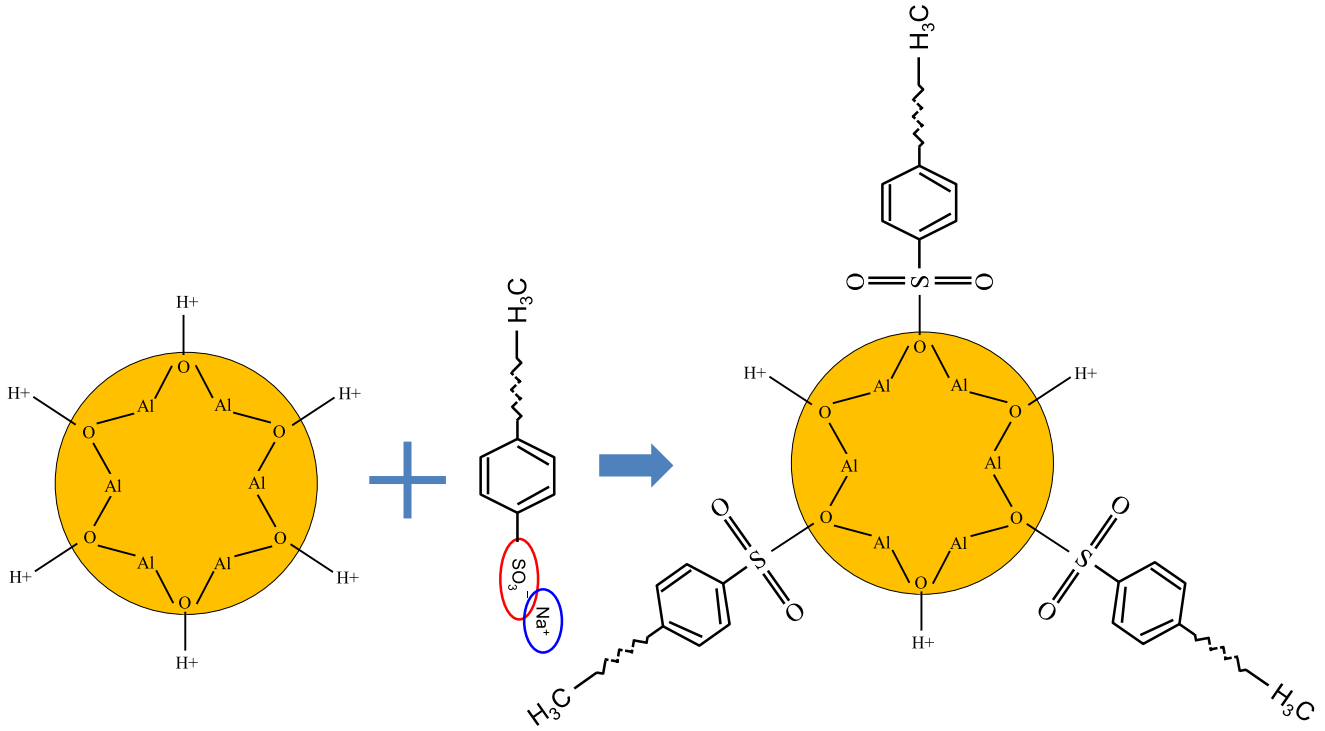

FIGURE 10. The adsorption of SDBS surfactant on the surface of Al_2O_3 nanoparticles.

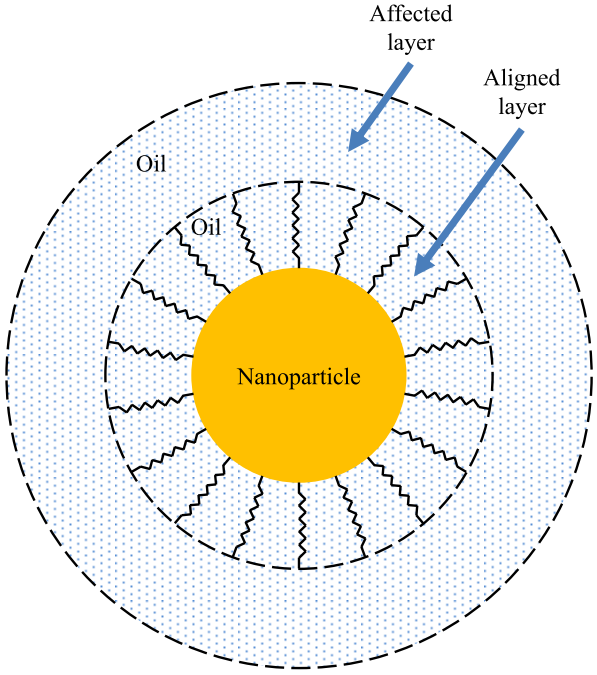

FIGURE 11. The structure of interfacial zone around nanoparticles in cottonseed oil.

an extended part with consideration of surfactant effect. It is clear that there is a decrement in the relative permittivity due to orientational polarization after surfactant treatment compared to without surfactant treatment at a given temperature and filler levels of nanoparticles. As discussed earlier, this is due to the effect of aligned layer that is difficult to polarize.

X. CONCLUSION

Effect of interfacial zone on dielectric properties of cottonseed oil based Al_2O_3DNFs was investigated. Detailed characterization of Al_2O_3 nanoparticles and methodology adopted for the preparation of DNFs were presented. A relative permittivity model of DNFs considering surfactant polarization was proposed. Experimental relative permittivity results of DNFs at varying temperature were investigated. Relative permittivities of proposed model were compared with experimental results. Effect of interfacial zone on dissipation factor and AC BDV were also discussed with the help of experimental results and corresponding physical mechanisms. The conclusions made are as follows:

1. The relative permittivity of Al_2O_3 DNFs increased with the increase in the weight percentage of NPs. This was explained considering internal polarization of NPs and orientational polarization of charged NPs.
2. The relative permittivity of Al_2O_3 DNFs decreased with the increase in temperature, which is a similar trend to that obtained in literature.
3. From the proposed model, it was found that surfactant contributes for orientational polarization of Al_2O_3 nanoparticles in Clausius-Mossotti equation for the relative permittivity of DNFs.
4. From the proposed model, the relative permittivity of DNFs was found independent of the diameter of nanoparticles (from the range 2a = 15nm to 25nm) and

the thickness of surfactant (from the range d = 1.5nm to 3.0nm), but instead it was highly dependent on the number of nanoparticles per unit volume, thus indirectly depends on the dispersion state.

5. Relative permittivities of proposed model were almost in line with experimental results, at a given weight percentage of Al_2O_3 NPs and at a given temperature. The highest percentage difference between experimental and model results was 6.16%.
6. The dissipation factor of DNFs decreased with the increase in weight percentage of Al_2O_3 NPs due to the increase of relative permittivity that clarified from the proposed model and the decrease of dielectric loss that provided by charge trapping of nanoparticles and their interfaces.
7. In the current study, concentrations up to 0.05 wt% were found to be below or equal to the critical concentration. Therefore, the mean AC BDV of surfactant driven nanofluid was incremental with the weight percentage of Al_2O_3 NPs due to the increase in trapping depth. Maximum AC BDV was measured as 46.2 kV corresponding to a percentage enhancement of about 23%.

REFERENCES

[1] M. M. M. Salama, D.-E.-A. Mansour, M. Daghrah, S. M. Abdelkasoud, and A. A. Abbas, "Thermal performance of transformers filled with environmentally friendly oils under various loading conditions," *Int. J. Electr. Power Energy Syst.*, vol. 118, Jun. 2020, Art. no. 105743.

[2] U. Khaled and A. Beroual, "Lightning impulse breakdown voltage of synthetic and natural ester liquids-based Fe3O4, Al_2O_3 and SiO_2 nanofluids," *Alexandria Eng. J.*, vol. 59, no. 5, pp. 3709–3713, Oct. 2020.

[3] F. Ahmad, A. A. Khan, Q. Khan, and M. R. Hussain, "State-of-art in nano-based dielectric oil: A review," *IEEE Access*, vol. 7, pp. 13396–13410, 2019.

[4] M. Nazari, M. H. Rasoulifard, and H. Hosseini, "Dielectric breakdown strength of magnetic nanofluid based on insulation oil after impulse test," *J. Magn. Magn. Mater.*, vol. 399, pp. 1–4, Feb. 2016.

[5] S. Aberoumand and A. Jafarimoghaddam, "Tungsten (III) oxide (WO_3)–silver/transformer oil hybrid nanofluid: Preparation, stability, thermal conductivity and dielectric strength," *Alexandria Eng. J.*, vol. 57, no. 1, pp. 169–174, Mar. 2018.

[6] P. Bartko, M. Rajňák, R. Cimbala, K. Paulovičová, M. Timko, P. Kopčanský, and J. Kurimský, "Effect of electrical polarity on dielectric breakdown in a soft magnetic fluid," *J. Magn. Magn. Mater.*, vol. 497, Mar. 2020, Art. no. 166007.

[7] M. Rafiq, L. Chengrong, and Y. Lv, "Effect of Al_2O_3 nanorods on dielectric strength of aged transformer oil/paper insulation system," *J. Mol. Liquids*, vol. 284, pp. 700–708, Jun. 2019.

[8] C. Olmo, C. Méndez, F. Ortiz, F. Delgado, and A. Ortiz, "Titania nanofluids based on natural ester: Cooling and insulation properties assessment," *Nanomaterials*, vol. 10, no. 4, p. 603, Mar. 2020.

[9] S. S. Dessouky, D.-E.-A. Mansour, M. Shaban, and S. A. M. Abdelwahab, "Insulation performance enhancement of aged current transformers using nanofluids," *Int. J. Electr. Power Energy Syst.*, vol. 126, Mar. 2021, Art. no. 106613.

[10] M. Meunier, N. Quirke, and A. Aslanides, "Molecular modeling of electron traps in polymer insulators: Chemical defects and impurities," *J. Chem. Phys.*, vol. 115, no. 6, pp. 2876–2881, Aug. 2001.

[11] T. Takada, Y. Hayase, Y. Tanaka, and T. Okamoto, "Space charge trapping in electrical potential well caused by permanent and induced dipoles," in *Proc. Annu. Rep.-Conf. Electr. Insul. Dielectr. Phenomena*, Oct. 2007, pp. 417–420.

[12] M. R. Hussain, Q. Khan, A. A. Khan, S. S. Refaat, and H. Abu-Rub, "Dielectric performance of magneto-nanofluids for advancing oil-immersed power transformer," *IEEE Access*, vol. 8, pp. 163316–163328, 2020.

[13] D. Li and J. Li, "Effective dielectric constant of plasmonic nanofluid containing core-shell nanoparticles," *Plasmonics*, vol. 14, no. 1, pp. 263–270, Feb. 2019.

[14] J. Miao, M. Dong, M. Ren, X. Wu, L. Shen, and H. Wang, "Effect of nanoparticle polarization on relative permittivity of transformer oil-based nanofluids," *J. Appl. Phys.*, vol. 113, no. 20, May 2013, Art. no. 204103.

[15] M. Rafiq, M. Shafique, A. Azam, and M. Ateeq, "Transformer oil-based nanofluid: The application of nanomaterials on thermal, electrical and physicochemical properties of liquid insulation—A review," *Ain Shams Eng. J.*, vol. 12, no. 1, pp. 555–576, Mar. 2021.

[16] J. Li, B. Du, F. Wang, W. Yao, and S. Yao, "The effect of nanoparticle surfactant polarization on trapping depth of vegetable insulating oil-based nanofluids," *Phys. Lett. A*, vol. 380, no. 4, pp. 604–608, Feb. 2016.

[17] C. Choi, H. S. Yoo, and J. M. Oh, "Preparation and heat transfer properties of nanoparticle-in-transformer oil dispersions as advanced energy-efficient coolants," *Current Appl. Phys.*, vol. 8, no. 6, pp. 710–712, Oct. 2008.

[18] E. G. Atiya, D.-E.-A. Mansour, R. M. Khattab, and A. M. Azmy, "Dispersion behavior and breakdown strength of transformer oil filled with TiO_2 nanoparticles," *IEEE Trans. Dielectr. Electr. Insul.*, vol. 22, no. 5, pp. 2463–2472, Oct. 2015.

[19] R. A. Farade, N. I. A. Wahab, D.-E.-A. Mansour, N. B. Azis, J. B. Jasni, V. Veerasamy, M. Thirumeni, A. X. R. Irudayaraj, and A. S. Murthy, "Investigation of the effect of sonication time on dispersion stability, dielectric properties, and heat transfer of graphene based green nanofluids," *IEEE Access*, vol. 9, pp. 50607–50623, 2021.

[20] D. Liu, Y. Zhou, Y. Yang, L. Zhang, and F. Jin, "Characterization of high performance AIN nanoparticle-based transformer oil nanofluids," *IEEE Trans. Dielectr. Electr. Insul.*, vol. 23, no. 5, pp. 2757–2767, Oct. 2016.

[21] M. Rajňák, J. Kurimský, R. Cimbala, Z. Čonka, P. Bartko, M. Šuga, K. Paulovičová, J. Tóthová, M. Karpets, P. Kopčanský, and M. Timko, "Statistical analysis of AC dielectric breakdown in transformer oil-based magnetic nanofluids," *J. Mol. Liquids*, vol. 309, Jul. 2020, Art. no. 113243.

[22] D.-E.-A. Mansour and E. G. Atiya, "Application of UV/Vis spectroscopy to assess the stability of oil-based nanofluids," in *Proc. IEEE Conf. Electr. Insul. Dielectr. Phenomena (CEIDP)*, Oct. 2016, pp. 671–674.

[23] T. Tanaka, M. Kozako, N. Fuse, and Y. Ohki, "Proposal of a multi-core model for polymer nanocomposite dielectrics," *IEEE Trans. Dielectr. Electr. Insul.*, vol. 12, no. 4, pp. 669–681, Aug. 2005.

[24] R. Smith, C. Liang, M. Landry, J. Nelson, and L. Schadler, "The mechanisms leading to the useful electrical properties of polymer nanodielectrics," *IEEE Trans. Dielectr. Electr. Insul.*, vol. 15, no. 1, pp. 187–196, Feb. 2008.

[25] R. Kochetov, T. Andritsch, P. H. F. Morshuis, and J. J. Smit, "Anomalous behaviour of the dielectric spectroscopy response of nanocomposites," *IEEE Trans. Dielectr. Electr. Insul.*, vol. 19, no. 1, pp. 107–117, Feb. 2012.

[26] D. Zhu, X. Li, N. Wang, X. Wang, J. Gao, and H. Li, "Dispersion behavior and thermal conductivity characteristics of Al_2O_3–H2O nanofluids," *Current Appl. Phys.*, vol. 9, no. 1, pp. 131–139, Jan. 2009.

[27] M. K. Dowd, "Cottonseed oil," in *Vegetable Oils in Food Technology: Composition, Properties and Uses*, F. D. Gunstone, Ed., 2nd ed. Oxford, U.K.: Blackwell, 2011, pp. 199–224.

[28] A. Siger, M. Nogala-Kalucka, and E. Lampart-Szczapa, "The content and antioxidant activity of phenolic compounds in cold-pressed plant oils," *J. Food Lipids*, vol. 15, no. 2, pp. 137–149, May 2008.

[29] R. A. Farade, N. I. B. A. Wahab, D.-E.-A. Mansour, N. B. Azis, J. Jasni, N. R. Banapurmath, and M. E. M. Soudagar, "Investigation of the dielectric and thermal properties of non-edible cottonseed oil by infusing h-BN nanoparticles," *IEEE Access*, vol. 8, pp. 76204–76217, 2020.

[30] R. A. Farade, N. I. A. Wahab, D.-E.-A. Mansour, N. B. Azis, J. B. Jasni, M. E. M. Soudagar, and V. Siddappa, "Development of graphene oxide-based nonedible cottonseed nanofluids for power transformers," *Materials*, vol. 13, no. 11, p. 2569, Jun. 2020.

[31] J. Jacob, P. Preetha, and T. K. Sindhu, "Stability analysis and characterization of natural ester nanofluids for transformers," *IEEE Trans. Dielectr. Electr. Insul.*, vol. 27, no. 5, pp. 1715–1723, Oct. 2020.

[32] S. O. Kasap, *Principles of Electronic Materials and Devices*, 4th ed. New York, NY, USA: McGraw-Hill, 2018.
[33] A. Thabet, S. A. Shaaban, and M. Allam, "Enhancing dielectric constant of transformer oils using multi-nanoparticles technique under thermal conditions," in *Proc. 18th Int. Middle East Power Syst. Conf. (MEPCON)*, Dec. 2016, pp. 220–225.
[34] M. M. Bhunia, K. Panigrahi, S. Das, K. K. Chattopadhyay, and P. Chattopadhyay, "Amorphous graphene – transformer oil nanofluids with superior thermal and insulating properties," *Carbon*, vol. 139, pp. 1010–1019, Nov. 2018.
[35] V. Mentlik, P. Trnka, J. Hornak, and P. Totzauer, "Development of a biodegradable electro-insulating liquid and its subsequent modification by nanoparticles," *Energies*, vol. 11, no. 3, p. 508, Feb. 2018.
[36] M. L. Karon and A. M. Altschul, "Effect of moisture and of treatments with acid and alkali on rate of formation of free fatty acids in stored cottonseed," *Plant Physiol.*, vol. 19, no. 2, pp. 310–325, Apr. 1944.
[37] S. Kittaka, "Isoelectric point of Al_2O_3, Cr_2O_3 and Fe_2O_3. I. Effect of heat treatment," *J. Colloid Interface Sci.*, vol. 48, no. 2, pp. 327–333, Aug. 1974.
[38] D.-E.-A. Mansour, A. M. Elsaeed, and M. A. Izzularab, "The role of interfacial zone in dielectric properties of transformer oil-based nanofluids," *IEEE Trans. Dielectr. Electr. Insul.*, vol. 23, no. 6, pp. 3364–3372, Dec. 2016.

RIZWAN A. FARADE received the B.E. degree in electrical and electronics engineering from Visvesvaraya Technological University, Belgaum, India, in 2005, and the M.Tech. degree in power electronics from Jawaharlal Nehru Technological University Hyderabad, India, in 2013. He is currently pursuing the Ph.D. degree in electrical and electronics engineering with University Putra Malaysia, Serdang, Malaysia. Since 2009, he has been a Lecturer and an Assistant Professor in India's diploma and undergraduate programs. Since 2014, he has been with Kalsekar Technical Campus, New Mumbai, India, as an Assistant Professor in an undergraduate program. His research interests include dielectric fluids, power systems, and nano biodiesel.

NOOR IZZRI ABDUL WAHAB (Senior Member, IEEE) received the B.Sc. degree in electrical and electronic engineering from the University of Manchester Institute of Science and Technology (UMIST), U.K., in 1998, the M.Sc. degree in electrical power engineering from Universiti Putra Malaysia (UPM), in 2002, and the Ph.D. degree in electrical, electronic and system engineering from Universiti Kebangsaan Malaysia (UKM), in 2010. He is currently an Associate Professor with the Department of Electrical and Electronic Engineering, Faculty of Engineering, UPM. He is the Founding Member of the Advanced Lightning, Power and Energy Research Centre (ALPER), UPM. He is a Registered Chartered Engineer (CEng), a Professional Engineer (Ir.), and a member of The Institution of Engineers Malaysia (IEM). His research interests include power system stability, application of AI in power systems, and power quality.

DIAA-ELDIN A. MANSOUR (Senior Member, IEEE) was born in Tanta, Egypt, in December 1978. He received the B.Sc. and M.Sc. degrees in electrical engineering from Tanta University, Tanta, Egypt, in 2000 and 2004, respectively, and the Ph.D. degree in electrical engineering from Nagoya University, Nagoya, Japan, in 2010. Since 2000, he has been with the Department of Electrical Power and Machines Engineering, Faculty of Engineering, Tanta University, Egypt, where he is currently working as a Full Professor and the Director of the High Voltage and Superconductivity Laboratory. Since 2010, he has been a Foreign Researcher for three months with the EcoTopia Science Institute, Nagoya University. His research interests include high-voltage engineering, renewable energy, smart grids, nanodielectrics, and applied superconductivity. He received the best presentation award two times from IEE of Japan, in 2008 and 2009. He also received the Prize from the Egyptian Academy of Scientific Research and Technology, in 2013, Tanta University Encouragement Award, in 2017, the Egypt-State Encouragement Award in the field of engineering sciences, in 2018, and Tanta University Citations Award, in 2021. In 2020, he has been listed among the world's top 2% scientists by Stanford University, USA.

NORHAFIZ B. AZIS (Senior Member, IEEE) received the B.Eng. degree in electrical and electronic engineering from Universiti Putra Malaysia, Malaysia, in 2007, and the Ph.D. degree in electrical power engineering from The University of Manchester, U.K., in 2012. He is currently an Associate Professor with the Department of Electrical and Electronic Engineering, Universiti Putra Malaysia. His research interests include in-service aging of transformer insulation, condition monitoring, asset management, and alternative insulation materials for transformers.

JASRONITA BT. JASNI (Senior Member, IEEE) received the B.Eng. and M.Eng. degrees in electrical engineering from Universiti Teknologi Malaysia, Johor, Malaysia, in 1998 and 2001, respectively, and the Ph.D. degree in electrical power engineering from Universiti Putra Malaysia, Selangor, Malaysia, in 2010. From 1998 to 1999, she was a System Engineer. From 1999 to 2001, she worked as a Tutor with the Department of Electrical and Electronics Engineering, Faculty of Engineering, Universiti Putra Malaysia, where she started working as a Lecturer, in 2001. She is currently an Associate Professor with the Department of Electrical and Electronics Engineering, Faculty of Engineering, Universiti Putra Malaysia. Her research interests include power systems, renewable energy, and lightning protection. She has received several awards and recognitions for her work and researches including the Excellent in Service Award and the Excellent in Teaching Award from the Universiti Putra Malaysia, and the Bronze Medal in Malaysia Technology Expo.

VEERAPANDIYAN VEERASAMY (Graduate Student Member, IEEE) received the bachelor's degree in electrical and electronics engineering from Panimalar Engineering College, India, in 2013, and the Master of Engineering degree in power systems engineering from the Government College of Technology, India, in 2015. He is currently pursuing the Ph.D. degree in power systems with Universiti Putra Malaysia, Malaysia. Since 2015, he has been working as an Assistant Professor with the Department of Electrical and Electronics Engineering, Rajalakshmi Engineering College, India. His research interests include the design of robust controllers for power system application, fault classification, and power system monitoring.

ARANGARAJAN VINAYAGAM (Member, IEEE) received the Ph.D. degree in PV integrated microgrid power system from Deakin University, Australia. He is currently working as a Visiting Professor with the Electrical and Electronics Engineering Department, New Horizon College of Engineering, Bangaluru, India. He has more than 15 years of industrial experience in the field of power plant industry and Renewable Energy Technologies. He has additional Academic experience (teaching and research) covering the area of smart grid and microgrid power system, renewable energy technologies, power generation and distribution control, distributed generation sources, and power quality. He has published more than 30 research articles in reputed journals, book chapters, and international conferences. His research interests include the development of smart microgrid power system with integrated solar PV and energy storage facility, extensive analysis of power quality, and electric faults in microgrid and large grid power system networks.

BANDANAWAZ M. KOTIYAL was born in Bijapur, India, in 1979. He received the B.Tech. degree in electronics and communication engineering from Karnataka University Dharwad (KUD), Karnataka, in 2001, and the M.Tech. degree in digital communication engineering from Visvesvaraya Technological University (VTU), Karnataka, in 2010.

T. M. YUNUS KHAN received the master's degree from Visvesvarayya Technological University (VTU), Belagavi, and the Ph.D. degree from the University of Malaya. He is currently working as an Assistant Professor with the Department of Mechanical Engineering, King Khalid University, Saudi Arabia. Having 19 years of teaching and research experience, he has published more than 85 research articles in reputed ISI (Thompson Reuters) indexed peer-reviewed international journals and conferences so far. He has delivered keynote addresses in international conferences and seminars.